ChemComm

Photocatalytic aerobic oxidation of benzylic alcohols and concomitant hydrogen peroxide production

Journal:	*ChemComm*
Manuscript ID	CC-COM-08-2022-004351.R3
Article Type:	Communication

COMMUNICATION

Photocatalytic Aerobic Oxidation of Benzylic Alcohols and Concomitant Hydrogen Peroxide Production

Avik Bhattacharjee, Aireth R. LaVigne, Serena M. Frazee, Tyler L. Herrera, and Theresa M. McCormick*

Received 00th January 20xx,
Accepted 00th January 20xx

DOI: 10.1039/x0xx00000x

The photochemical oxidation of benzylic alcohols using *N*-hydroxyphthalimide (NHPI) catalysts, with Rose Bengal as a singlet oxygen photosensitizer, and the production of hydrogen peroxide (H_2O_2) under metal-free conditions is presented. Computational and experimental investigations support $^1O_2$ as the oxidant that converts NHPI to the active radical intermediate phthalimide-*N*-oxyl (PINO). This is a green alternative to current methods of H_2O_2 production.

Aerobic oxidation using transition metal catalysts is widely used for the transformation of organic molecules.[1–4] Photocatalytic and metal-free aerobic oxidation is an emerging field in the area of sustainable chemical research. Organo-catalysts are desirable due to their high reactivity and tunability. Use of *N*-hydroxyphthalimide (NHPI) as an organic oxidation catalyst has been reported in literature for a variety of substrates, usually under thermal conditions, with metal activators.[5–7] Recent reviews have highlighted the use of N-hydroxyl radicals in organic reactions.[8–10] In a previously published report on aerobic oxidation of alcohols with NHPI using thermochemical conditions, Ishii *et al.* reported H_2O_2 generation in this reaction.[11]

H_2O_2 has widespread use in several laboratory and industrial processes and has many household uses.[3,9,10] Recent reports reveal that H_2O_2 can also act as a sustainable, carbon-neutral fuel in an electrochemical fuel cell, producing only water as the waste material.[3,14] However, the current method of H_2O_2 production utilizes the energy intensive Anthraquinone Process that uses H_2 and O_2 and an expensive Pd-catalyst.[15,16] Here we report a simple strategy to achieve aerobic oxidation of benzylic alcohols (benzhydrol, and benzyl alcohol) in metal-free and photocatalytic conditions and the concomitant reduction of oxygen to H_2O_2. Coupled to a photochemical reaction, this is a green method for H_2O_2 production.

Oxidation reactions using NHPI are reported to follow a radical mechanism.[5,6] Homolytic cleavage of the NO-H bond generates the phthalimide-*N*-oxyl (PINO) radical (**Scheme 1**). PINO reacts with substrate to generate a benzylic radical that reacts with O_2 to form a metastable hydroxy (perhydroxy) intermediate. Finally, hydroperoxyl leaves as H_2O_2 generating a carbonyl compound as the final product. However, under thermochemical conditions cobalt and/or manganese co-catalysts are often used to initiate H-atom abstraction from NHPI to produce the active radical species, PINO. Thus, any H_2O_2 produced in these systems decompose under these reaction-conditions; attempts to isolate H_2O_2 have not been reported.[11] Furthermore, thermal reactions require elevated temperatures (70-90 °C) where PINO is prone to decomposition.[17–19] Hence, utilizing low-temperature photochemical reactions with no metal co-catalysts will allow both the oxidized products and H_2O_2 to be isolated.

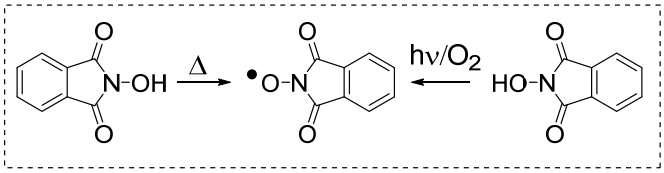

Scheme 1 Thermal and photochemical production of PINO from NHPI.

Photocatalytic oxidation of the α-C of unsaturated hydrocarbons has been reported with NHPI as a radical organo-catalyst where CdS acts as a photo-redox catalyst to generate PINO and to reduce oxygen to superoxide.[20] Similarly, the excited-state of graphitic-carbon-nitride (g-C_3N_4) can activate O_2 to superoxide, which promotes hydrogen abstraction from NHPI, generating PINO[21–23] Photocatalysis through PINO generation has also been reported for heterogenous systems using α-Fe_2O_3 or TiO_2.[24,25] This differs from our proposed reaction mechanism where $^1O_2$ is the ROS. In a recent paper by Chen *et al.*, Rose Bengal was used as a photosensitizer for the synthesis of β-oxy alcohols.[26] This work indicates that PINO is generated by the sensitized $^1O_2$, however this reaction is not catalytic since PINO is consumed during the reaction.

Our novel strategy using visible light provides the oxidation products in comparable yield to thermal conditions. Diphenylmethanol (**1,** 5 mmol) was reacted with molecular O_2 in the presence of NHPI (5 mol%) catalyst and a photosensitizer (Rose Bengal, (**RB**)) in 5 mL acetonitrile (ACN) under white light irradiation at room temperature for 72 hours to afford benzophenone (**3**) and H_2O_2 (**2**) as identified by ^{1}H NMR (**Figure 1a**, Supporting Information **Figure S1 and 2**). The NMR yields are

[a] *Portland State University, Department of Chemistry, Portland, OR, 97201*
Electronic Supplementary Information (ESI) available: [details of any supplementary information available should be included here]. See DOI: 10.1039/x0xx00000x

73% for benzophenone (**3**) and 57% for hydrogen peroxide (**2**). When a primary alcohol, phenylmethanol (**4**), was oxidized employing the same reaction conditions benzaldehyde (**5**), 29%; and a trace amount of benzoin, 3% along with H_2O_2 (20%) were identified **Figure 1b,** Supporting Information **Figure S3 and 4**). Oxidation of (E)- cinnamyl alcohol and (±)-phenylethyl alcohol resulted in low but measurable yields (5% and 8% respectively, after 72 h) (Supporting Information Table S1). The higher yield of the oxidation products for benzophenone can be attributed to the higher stability of the corresponding benzylic radical intermediate.

To evaluate the effect of each of the components of the reaction we ran a series of control experiments and screened them for the production of H_2O_2 using peroxide test-strips (**Table 1**). The positive control reaction (Entry 1) was run using 5 mmol **1**, and 10 mol% NHPI in 5 mL of a 10^{-4} M **RB** solution in acetonitrile. The reaction flask was sealed with a balloon filled with oxygen gas. The reaction was stirred vigorously (1500 rpm) for 72 hours while being irradiated with a 24 W white light LED strip coiled in a 12-inch metal tube. Hydrogen peroxide was separated from the organic layer into the aqueous layer by liquid-liquid extraction with 5 mL toluene and 5 mL of water. A blue coloration of the peroxide test-strip indicated the presence of H_2O_2 in the aqueous work-up of the reaction. To rule out a false positive indication on the test strips caused by other types of peroxides or reactive oxygen species (ROS), we performed absorption studies with a selective titanium(IV)-porphyrin dye, oxo[5,10,15,20-tetra(4-pyridyl)porphyrinato]titanium (IV), $[TiO(TPyPH_4)]^{4+}$ and observed a shift in the absorption peak at 432 nm to 445 nm confirming the presence of $[TiO_2(TPyPH_4)]^{4+}$ (Supporting Information **Figure S5**).[27] Thus, a color change on the test strip was used to indicate a positive control for the reactions, and if no hydrogen peroxide was detected we assumed there was no reaction. In absence of NHPI (Entries 2, and 3), or light (Entries 3, 6, and 7) no H_2O_2 was detected. No H_2O_2 was detected if no alcohol was included (Entry 4). To investigate the role of temperature two reactions were ran at 0 °C in the presence, and absence of light. The reaction tested positive for H_2O_2 production at 0 °C in the presence of light (Entry 8), however no H_2O_2 was observed under dark reaction conditions (Entry 9), likewise the reaction didn't proceed without **RB** The reaction was monitored with irradiation for 1 day, followed by dark for 1 day, and then irradiation for 1 day. The reaction only proceeded while it was irradiated and the overall yield after this 72 h experiment was similar to only being run for 48 h, the total time of irradiation (Supporting Information **Figure S6**).

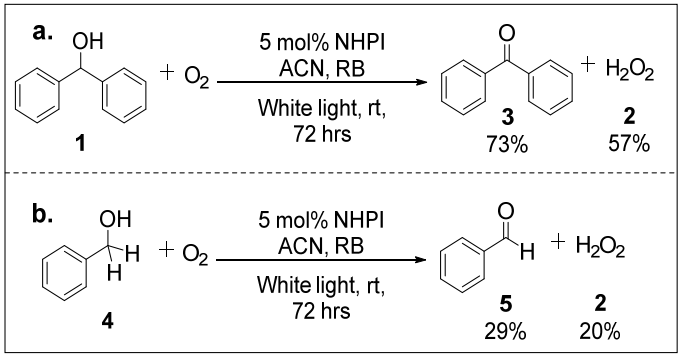

Figure 1. Aerobic oxidation of benzylic alcohols to hydrogen peroxide and the corresponding carbonyl compounds: a. photocatalytic oxidation of secondary alcohol benzhydrol, b. photocatalytic oxidation of primary alcohol phenylmethanol.

Table 1 Control experiments by varying the reaction conditions. The '+' sign denotes the presence and the '-' sign denotes the absence of the indicated condition. The blue coloration on the test strips indicates the production of H_2O_2 denoted by a '+' sign, whereas a '-' sign denotes no color change on the test strip indicating no H_2O_2 production. Reactions were run for 24 h with Rose Bengal as the photosensitizer.

Entry	[1] mmol	[NHPI] mol%	O_2	Light	Temperature (°C)	H_2O_2 test
1	5	10	+	+	25	+
2	5	-	+	+	25	-
3	5	-	+	-	25	-
4	-	10	+	+	25	-
5	5	10	-	+	25	-
6	5	10	+	-	25	-
7	5	10	+	-	25	-
8	5	10	+	+	0	+
9	5	10	+	-	0	-

The oxidation products (**2** and **3**) were found to be stable under the reaction conditions over 18 days by ^{1}H NMR (**Figure 2**, Supporting Information **Figure S7**). Around 12 days of irradiation time the reaction reaches the maximum yield at ~80% of **3** and ~57% of **2**. Iodometric titration of the extracted aqueous layer gave similar H_2O_2 yields as to those calculated by NMR. Separation and purification of **2** resulted in a 74% isolated yield after 7 days of irradiation.

The reaction conditions were optimized by running a three variable full factorial design of experiments (**Table 2**).[28] The variables considered in this study were concentration of the catalyst (NHPI in mol%), concentration of the photosensitizer (**RB** in M), and the irradiation time (in days). Using a full factorial design of experiment allows for reaction optimizations with few

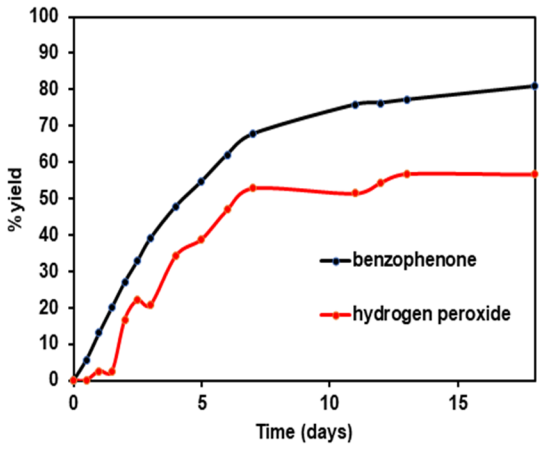

Figure 2. Yield of the oxidation products (benzophenone, and hydrogen peroxide) measured over a period of 18 days using ^{1}H NMR spectroscopy of the reaction mixture.

experiments, and accounts for interacting variables. The % yield was calculated integrating product peaks in the ^{1}H NMR with respect to an internal standard, ethylene carbonate. After calculating the main and interaction effects of the variables it was observed the yield was maximized at lower levels of catalyst loading (5 mol%) and photosensitizer concentration (1×10^{-4} M) but longer irradiation time (3 days). In the previous work by Ishii *et al.* in thermal condition 10 mol% catalyst-loading yielded maximum turnover.[11] In our photochemical conditions the better performance with a lower catalyst-loading can be

Table 2 Three variable full factorial optimization design for the photocatalytic aerobic oxidation of diphenylmethanol. The effect of catalyst concentration, photosensitizer concentration, and irradiation time were investigated for the optimization experiments.

Reaction	[NHPI] mol%	[RB] $\times10^{-4}$ M	Time (days)	%yield	
				3	**2**
1	10	4	2	10	6
2	5	1	1	4	-
3	15	1	1	3	1
4	5	7	1	5	1
5	15	7	1	5	1
6	5	1	3	77	50
7	15	1	3	21	14
8	5	7	3	26	6
9	15	7	3	22	15

attributed to more stable radical intermediates at lower temperatures minimizing catalyst degradation. The observation that longer irradiation time increases the product yield agrees with the ^{1}H NMR stability experiments and suggests slower aerobic oxidation kinetics and high energy of activation.[1,29]

To gain insight on the mechanism of the photocatalytic aerobic oxidation of benzhydrol to benzophenone using NHPI in presence of a photosensitizer, quenching experiments were run with the addition of different scavengers (Q) for intermediates (**Table 3**).[20] Addition of sodium azide as a singlet oxygen ($^1O_2$) scavenger entirely quenched the reaction. No oxidation products were observed after three days of irradiation. Addition of benzoquinone as a superoxide (O_2^-) scavenger lowered the yield. These two experiments together suggest the primary ROS responsible for the reaction is $^1O_2$ but that superoxide may be present and contributing to the reaction yield. We propose the **RB** sensitized singlet oxygen as the main ROS. This mechanism was further supported by generating $^1O_2$ from Li_2MoO_4 catalyzed decomposition of H_2O_2 without light. This reaction resulted in the oxidation products only in the presence of NHPI.

Table 3. Quenching experiments to investigate the nature of the reactive oxygen species (ROS) and the reaction intermediates.

Entry	Q	Q type	%+yield of 3
1	-	-	77
2	NaN_3	$^1O_2$	0
3	Benzoquinone	O_2^-	12
4	$(NH_4)_2C_2O_4$	hole	4
5	^{t}BuOH	radicals	19

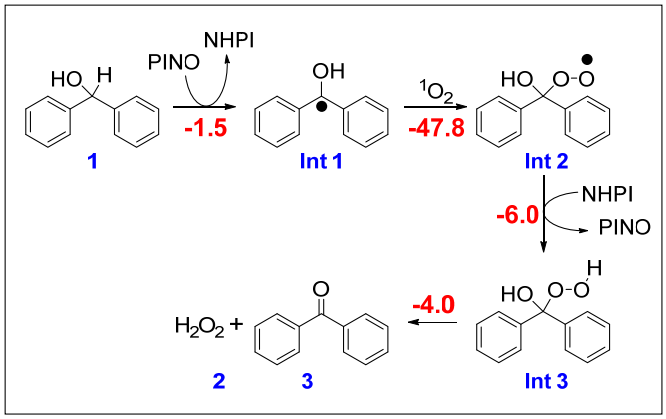

Scheme 2. Computationally investigated [M06-2X/6-311+G(d,p) in polarized acetonitrile solvation model] catalytic mechanism of aerobic oxidation of diphenylmethanol including the free energies of the intermediate steps (shown in blue).

The suppression of the yield of the oxidation products upon the addition of ammonium oxalate and *tert*-butyl alcohol suggests that the reaction is dependent on hole and radical intermediates, respectively. This observation further validates the lower yield of oxidation products for the primary alcohol. The benzylic radical intermediate has a lower stabilization for the primary alcohol when compared to the corresponding radical intermediate generated from the secondary alcohol, lowering the overall yield of the reaction.

A previously proposed mechanism using RB and NHPI includes reductive quenching of the excited RB*.[26] Subsequent regeneration of RB occurs from RB^+ getting an electron from deprotonated NHPI created by an added base. Since our reaction does not have a base to make deprotonated NHPI or an electron donor to regenerate the oxidized RB, this mechanism is not likely under these conditions Additionally, using methylene blue (**MB**) as the photosensitizer resulted in 4.5% production of **2** in 72 h. The lower yield is expected since the singlet oxygen quantum yield of MB is only 0.49 compared to 0.76 for RB.[30] Using this information, we propose that the photosensitizer makes singlet oxygen that reacts with NHPI to form PINO that initiates the radical oxidation reaction. The reaction pathway suggested by these experiments was explored using Density Functional Theory (DFT) calculations.

The geometries of the intermediates were optimized using M06-2X/6-311+G(d,p) method implementing an implicit polarized continuum solvation model for acetonitrile in Gaussian 09.[31,32] Three probable reaction combinations were modeled using $^1O_2$ and $^3O_2$, and $^2O_2^-$ to calculate the free energy change associated with the generation of PINO radical from NHPI (ΔG_{rxn}), which is the most crucial step in NHPI catalyzed aerobic oxidation (**Table 4**). PINO acts as the active catalyst that initiates the radical chain reaction by abstracting the methylene H atom of the secondary alcohol (**1**).

Unsurprisingly, reactions involving the more energetic $^1O_2$ is thermodynamically most favorable, characterized by the most negative free energy change value (Entry 2). However, the less positive Gibbs energy change corresponds to the reaction with superoxide (Entry 3). These results suggest that $^1O_2$ can react with NHPI to generate PINO. Direct reaction with ground state

$^3O_2$ was energetically most unfavorable as seen in DFT calculations (Entry 1).

Table 4 Different reaction combinations and calculated free energy changes (ΔG_{rxn}) for the formation of PINO.

Entry	Reaction Combinations	ΔG_{rxn} (kcal mol^{-1})
1	^{1}NHPI + $^3O_2$ → ^{2}PINO + ^{2}HOȮ	27.99
2	^{1}NHPI + $^1O_2$ → ^{2}PINO + ^{2}HOȮ	-9.57
3	^{1}NHPI + $^2O_2^-$ → ^{2}PINO + ^{2}HOȮ	12.07

The catalytic mechanism for the aerobic oxidation of **1** to **3** were modeled using the following steps (**Scheme 2**). The H atom abstraction by PINO from **1** to form the radical intermediate (Int 1) has a free energy of -1.5 kcal mol^{-1}. The second step of the catalytic cycle, formation of the hydroxy (perhydroxy) intermediate (Int 2), was modeled using both $^1O_2$ and $^3O_2$ as oxidants. DFT calculations reveal that formation of Int 2 is thermodynamically more favorable in the presence of $^1O_2$ (ΔG_{rxn} = -47.8 kcal mol^{-1}) than $^3O_2$ (-1.56 kcal mol^{-1}). However, since $^1O_2$ is a transient excited state, $^3O_2$ may be the the more likely reactive partner in this step. The computational results suggest either is possible. The metastable hydroxy (hydroperoxy) intermediate (Int 3) formation followed by the release of H_2O_2 (**2**) to form organic oxidation product **3**, have thermodynamic free energies of -6.0 kcal mol^{-1}, and -4.0 kcal mol^{-1}, respectively.

In summary, the use of NHPI to perform aerobic oxidation reactions addresses different challenges in the field of aerobic oxidation catalysis. This method is a greener alternative to most common alcohol oxidation reactions. NHPI is a simple organic compound, this will allow us to tune the efficiency through simple structural modifications. Photochemical oxidation can be performed at room temperature or lower. Most importantly, this method generates H_2O_2 as a value-added product. Due to the absence of any metal reactants and mild reaction conditions, the generated H_2O_2 will not be decomposed and can be extracted from the mixture with simple liquid-liquid extraction procedures. The catalytic mechanism of aerobic oxidation catalyzed by NHPI was explored through quenching experiments and supported by DFT calculations. These results show the potential of using an organocatalyst that is capable of oxidizing alcohols to H_2O_2 under photochemical conditions, which is of immense interest at both laboratory and industrial scale.

AB conducted experiments, set up the computational work, analysed data and wrote the first draft of the paper, AL, SF, and TH conducted experiments, TM designed experiments, secured funding, managed the project and wrote the manuscript.

There are no conflicts to declare

Funding. The calculations were done on the high-performance computing cluster at Portland State University which was purchased in part with the funds from National Science Foundation (grant DMS 1624776).

Notes and references

1 J. E. Bäckvall, *Modern Oxidation Methods*, 2005.
2 S. D. McCann and S. S. Stahl, *J. Am. Chem. Soc.*, 2016, **138**, 199.
3 S. Fukuzumi, Y. Yamada and K. D. Karlin, *Electrochim. Acta*, 2012, **82**, 493–511.
4 L. M. Mirica, X. Ottenwaelder and T. D. P. Stack, *Chem. Rev.*, 2004, **104**, 1013–1046.
5 F. Recupero and C. Punta, *Chem. Rev.*, 2007, **107**, 3800–3842.
6 L. Melone and C. Punta, *Beilstein J. Org. Chem.*, 2013, **9**, 1296.
7 G. Dobras, M. Sitko, M. Petroselli, M. Caruso, M. Cametti, C. Punta and B. Orlińska, *ChemCatChem*, 2020, **12**, 259–266.
8 M. A. Andrade and L. M. D. R. S. Martins, *EurJOC*, 2021, 4715.
9 E. V Tretyakov, V. I. Ovcharenko, A. O. Terent'ev, I. B. Krylov, T. V Magdesieva, D. G. Mazhukin and N. P. Gritsan, *Russ. Chem. Rev.*, 2022, **91**, RCR5025.
10 K. Chen, P. Zhang, Y. Wang and H. Li, *Green Chem.*, 2014, **16**, 2344–2374.
11 T. Iwahama, S. Sakaguchi and Y. Ishii, *Org. Process Res. Dev.*, 2000, **4**, 94–97.
12 S. Fukuzumi, Y. M. Lee and W. Nam, *Chem. - A Eur. J.*, 2018, **24**, 5016–5031.
13 S. Kato, J. Jung, T. Suenobu and S. Fukuzumi, *Energy Environ. Sci.*, 2013, **6**, 3756.
14 S. Fukuzumi and Y. Yamada, *ChemElectroChem*, 2016, **3**, 1978.
15 J. M. Campos-Martin, G. Blanco-Brieva and J. L. G. Fierro, *Angew. Chemie - Int. Ed.*, 2006, **45**, 6962–6984.
16 Q. Chang, P. Zhang, A. H. B. Mostaghimi, X. Zhao, S. R. Denny, J. H. Lee, H. Gao, Y. Zhang, H. L. Xin, S. Siahrostami, J. G. Chen and Z. Chen, *Nat. Commun.*, 2020, **11**, 1–9.
17 R. Amorati, M. Lucarini, V. Mugnaini, G. F. Pedulli, F. Minisci, F. Recupero, F. Fontana, P. Astolfi and L. Greci, *J. Org. Chem.*, 2003, **68**, 1747–1754.
18 C. Yang, L. A. Farmer, D. A. Pratt, S. Maldonado and C. R. J. Stephenson, *J. Am. Chem. Soc.*, 2021, **143**, 10324–10332.
19 K. U. Ingold and D. A. Pratt, *Chem. Rev.*, 2014, **114**, 9022–9046.
20 G. Zhao, B. Hu, G. W. Busser, B. Peng and M. Muhler, *ChemSusChem*, 2019, **12**, 2795–2801.
21 F. Li, S. Tang, Z. Tang, L. Ye, H. Li, F. Niu and X. Sun, *Catal. Letters*, 2021, **151**, 17–26.
22 P. Zhang, Y. Wang, J. Yao, C. Wang, C. Yan, M. Antonietti and H. Li, *Adv. Synth. Catal.*, 2011, **353**, 1447–1451.
23 P. Zhang, J. Deng, J. Mao, H. Li and Y. Wang, *Chinese J. Catal.*, 2015, **36**, 1580–1586.
24 C. Zhang, Z. Huang, J. Lu, N. Luo and F. Wang, *J. Am. Chem. Soc.*, 2018, **140**, 2032–2035.
25 I. B. Krylov, E. R. Lopat, I. R. Subbotina, G. I. Nikishin, B. Yu and A. O. Terent, 2021, **42**, 1700–1711.
26 M. Z. Zhang, J. Tian, M. Yuan, W. Q. Peng, Y. Z. Wang, P. Wang, L. Liu, Q. Gou, H. Huang and T. Chen, *Org. Chem. Front.*, 2021, **8**, 2215–2223.
27 C. Matsubara, N. Kawamoto and K. Takamura, *Analyst*, 1992, **117**, 1781–1784.
28 J. E. C. Rolf Carlson, *Design and optimization in organic synthesis*, Elsevier, 2005.
29 Y. Deng, G. Zhang, X. Qi, C. Liu, J. T. Miller, A. J. Kropf, E. E. Bunel, Y. Lan and A. Lei, *Chem. Commun.*, 2015, **51**, 318–321.
30 L. V. Lutkus, S. S. Rickenbach and T. M. McCormick, *J. Photochem. Photobiol. A Chem.*, 2019, **378**, 131–135.
31 D. J. Frisch, M. J.; et. al, *Gaussian 09*, Gaussian, Inc., Wallingford CT, Revision D., 2009.
32 C. J. Cramer and D. G. Truhlar, *Phys. Chem. Chem. Phys.*, 2009, **11**, 10757–10816.